Journal of Ceramic Processing Research. Vol. 15, No. 3, pp. 167~172 (2014)

J O U R N A L O F
Ceramic Processing Research

Dynamics processes between Sm^{2+}, Sm^{3+} and color centers in KY_3F_{10} : Sm crystals

Mitsuo Yamaga[a,*], Shin-ichiro Tsuda[a], Jon-Paul R. Wells[b] and Thomas P. J. Han[c]

[a]*Department of Mathematical and Design Engineering, Gifu University, Gifu 501-1193, Japan*
[b]*Department of Physics and Astronomy, University of Canterbury, PB4800, Christchurch 8020, New Zealand*
[c]*Department of Physics, University of Strathclyde, Glasgow, G1 1XN, United Kingdom*

Three distinct Sm^{2+} impurity centers, a single Sm^{3+} impurity center, and a color center were identified in KY_3F_{10} with 1 mol.% of Sm ion dopant by their emission and excitation spectra in the vacuum ultraviolet (VUV), ultraviolet (UV), and visible regions. The excited states of the Sm^{2+} centers consisted of the lower ^5D_J (J = 0,1,2,3) multiplets and the higher lying $4f^55d$ excited states. VUV or UV excitation directly into the $4f^6 \rightarrow 4f^55d$ transitions of Sm^{2+} produced cascade emission from the metastable ^5D_J (J = 3,2,1,0) multiplets to the lowest ^7F_J (J = 0,1,2,3,4) multiplets at low temperatures. Energy transfer from Sm^{2+} to Sm^{3+} ions was observed in the excitation spectra of the Sm^{3+} emission. Excitation at 532 nm for a sample temperature of 300 K produced a broad emission band with a peak at 660 nm and sharp emission lines at 680, 692 and 738 nm, being due to Sm^{2+}. 532 nm irradiation for 30 minutes decreased the intensity of the broadband to one-quarter of the initial intensity and increased slightly the intensities of the sharp lines.

Key words: Phosphor, Samarium ions, Energy transfer, Dynamics of the excited states, KY_3F_{10}.

Introduction

Rare-earth ion doped materials have been extensively studied for use in important applications such as phosphors, lasers, scintillators, and optical memory devices [1]. Spectral hole burning was demonstrated in Sm^{2+}-doped borate glasses for frequency-selective optical memories [2]. Recently, intense ultraviolet (UV) upconversion emission of Tb^{3+} was observed in Tb^{3+}/Yb^{3+} codoped KY_3F_{10} (KYF) nanocrystals using a 976 nm pump laser for Yb^{3+} [3].

The KYF crystal is a cubic compound with space group O_h^5 [4]. Potassium ions occupy eight corners of a cubic cell, whereas yttrium ions are surrounded by eight fluorine ions forming a square-based antiprism. Trivalent rare-earth ions substitute for trivalent yttrium ions and thus reside on a site of C_{4v} point group symmetry. It is reported [5], that samarium ions in the KYF crystal doped with 0.1 molar percent samarium (KYF: 0.1%Sm) were observed to be present in the form of Sm^{2+} and Sm^{3+} despite substituting for trivalent yttrium ions. Substitution of Sm^{2+} for Y^{3+} ions required a charge compensator in the form of a nearby fluorine vacancy. Laser selective excitation identified three different Sm^{2+} sites that have been denoted by A, B and C [5]. The excited states of the dominant A and B centers consisted of the ^5D_J (J = 3,2,1,0) and (J = 2,1,0) multiplets, respectively, and the higher lying $4f^55d$ excited states, whereas the $4f^55d$ energy levels of the minor C center lied just above the $^5D_0$ multiplet [5]. The charge compensator lowered the energy levels of the $4f^55d$ excited states of Sm^{2+} [5].

Vacuum ultraviolet (VUV) and UV excitation directly into the $4f^6 \rightarrow 4f^55d$ transitions in KYF: 0.1%Sm produced cascade emission from the higher ^5D_J (J = 3,2,1,0) multiplets to the lowest ^7F_J (J = 0,1,2,3,4) multiplets [5, 6]. UV excitation also produced a broad emission band with a peak at 450 nm at low temperatures, which might be assigned to a defect center acting as charge compensators for Sm^{2+} centers [6]. The decay curves of the Sm^{2+} emission lines also exhibited energy transfer from the B to A centers of Sm^{2+} [6].

In this paper, we discuss temperature dependent energy transfer from the B and C centers of Sm^{2+} to the A center and from the A center to Sm^{3+} in KYF crystals doped with one molar percent of samarium (KYF: 1%Sm). A new broad emission band excited at 532 nm was observed at 300 K. It is tentatively assigned to either the $4f^55d \rightarrow 4f^6$ transitions of the C center or a color center in the form of an electron trapped at a fluorine vacancy. Optical bleaching of the broad emission band under continuous irradiation is discussed.

Experimental

KYF crystals were grown by the Bridgman-Stockbarger technique [5]. YF_3 and KF were mixed together in essentially stoichiometric amounts, taking into account the small amounts (1 mol.%) of SmF_3 to be added. The mixed charge was then placed in a graphite crucible. Good quality crystals were obtained

*Corresponding author:
Tel : +81-58-293-3052
Fax: +81-58-293-2415
E-mail: yamaga@gifu-u.ac.jp

by traversing the crucible at a rate of 0.8 mm/hr in the furnace through a temperature gradient.

Optical absorption and excitation spectra in the VUV, UV and visible regions were measured using the BL3B beam of the UVSOR facility in the Institute for Molecular Science. Crystals were attached on a cold copper finger in a liquid helium cryostat with a temperature control system. Emission spectra in the temperature range of 10-300 K were measured using an Acton SpectraPro-300i monochromator combined with a Roper Spec-10 Si-CCD detector cooled by liquid nitrogen. Emission and excitation spectra at 300 K were also measured using a JASCO FP-8600 spectrofluorometer. Optical bleaching measurement was carried out at 300 K using the second harmonics (532 nm) of a Spectra-Physics GCR100 Q-switched Nd : YAG pulsed laser as an excitation source.

Experimental Results

Figure 1 shows the optical absorption spectra observed in the range of 100-600 nm for KYF: 1%Sm at 10 and 300 K. The base line of the 10 K spectrum is shifted for clarity. The optical absorption spectrum at 10 K consists of several bands and lines, whereas the absorption bands and lines at 300 K are thermally broadened and unresolved. Comparatively broad features are not associated with Sm^{3+} ions in the KYF crystal, but assigned to the $4f^6(^7F_0) \rightarrow 4f^5 5d$ inter-configurational transitions of the Sm^{2+} ions [5]. As these optical transitions are parity-allowed by the electric dipole mechanism, they produce strong absorption bands [5]. Although the band gap energy of KYF cannot be estimated from the absorption spectra in Fig. 1, the value is expected to be comparable to those of other fluorides crystals, for example, CaF_2 (110 nm) [7] and $LiCaAlF_6$ (100 nm) [8]. As a consequence, the broad bands due to the $4f^6 \rightarrow 4f^5 5d$ transitions cover the range between 100 and 600 nm.

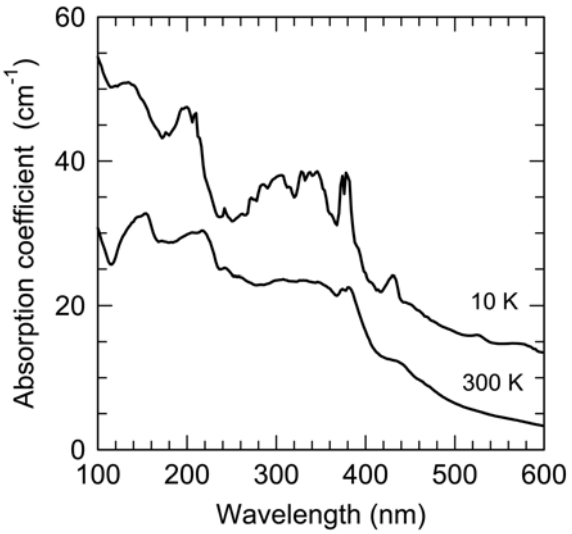

Fig. 1. Optical absorption spectra of KY_3F_{10} : 1%Sm observed at 10 and 300 K.

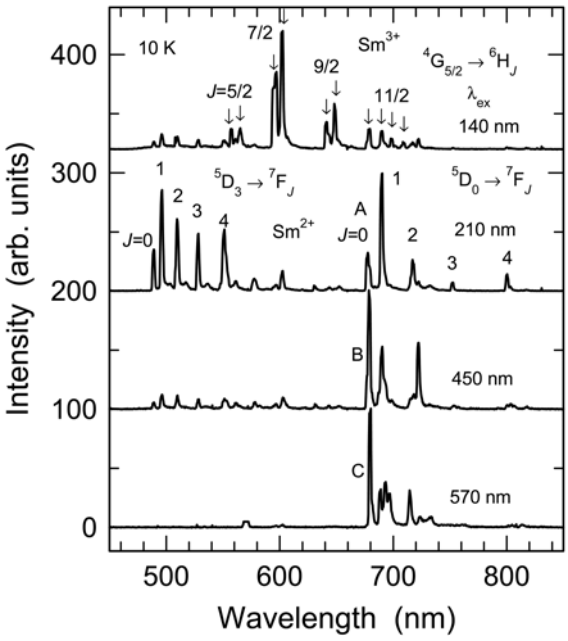

Fig. 2. Emission spectra excited at various wavelengths for KY_3F_{10} : 1%Sm at 10 K.

Figure 2 shows emission spectra excited at 140, 210, 450 and 570 nm for KYF: 1%Sm when measured at 10 K. All emission spectra are normalized by the maximum intensities and the base line of each spectrum is shifted for clarity. Emission excited at 140 nm has the typical Sm^{3+} emission pattern, consisting of four groups of sharp lines around 560, 600, 645 and 690 nm. The four groups are assigned to the $^4G_{5/2} \rightarrow {}^6H_J$ (J = 5/2,7/2,9/2,11/2) transitions of Sm^{3+}, respectively. The emission spectrum excited at 210 nm consists of two groups of sharp lines at 489, 496, 510, 529 and 551 nm and at 678, 690, 718, 752 and 800 nm. The latter pattern is a replica of the former pattern, being shifted towards low energy with an amount of 5,670 cm^{-1}. These groups are assigned to the $^5D_3 \rightarrow {}^7F_J$ (J = 0,1,2,3,4) and $^5D_0 \rightarrow {}^7F_J$ (J = 0,1,2,3,4) intra-$4f^6$ transitions of Sm^{2+} [5, 6]. This result indicates that the lowest excited states of the $4f^5 5d$ electronic configuration, corresponding to the absorption band with the peak at 430 nm in Fig. 1, lie above the $^5D_3$ multiplet and below the $^5D_4$ multiplet. In the same way, excitation at 450 and 570 nm changed positions, number and relative intensities of these sharp lines. These $^5D_0 \rightarrow {}^7F_J$ (J = 0,1,2,3,4) emission lines are denoted by A, B and C, as shown in Fig. 2 [5].

In order to examine the difference in the Sm^{2+} emission with various excitation wavelengths, the sharp lines around 680 and 690 nm due to the $^5D_0 \rightarrow {}^7F_0$ and $^5D_0 \rightarrow {}^7F_1$ transitions, respectively, were measured with higher resolution. Figure 3 shows the three distinct Sm^{2+} centers, denoted by A, B and C, being identified previously [5]. The $^5D_0 \rightarrow {}^7F_0$ lines for the B and C centers are red-shifted compared with that for the A

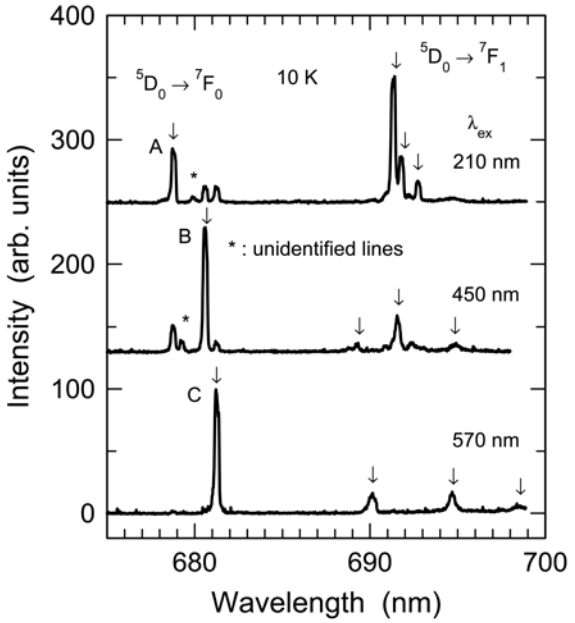

Fig. 3. Emission spectra measured with high resolution at various excitation wavelengths for KY_3F_{10} : 1%Sm at 10 K.

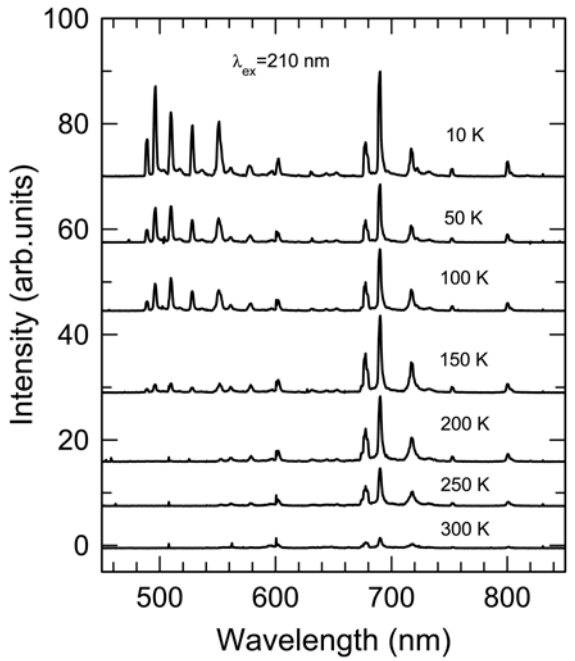

Fig. 4. Temperature dependent emission spectra of Sm^{2+} in KY_3F_{10} : 1%Sm with 210 nm excitation.

center, whereas their $^5D_0 \rightarrow {}^7F_1$ lines were clearly split into three components. The energy separation between the three lines increased in order of A, B and C. These results suggest that there exist, at least, three distinct Sm^{2+} centers in the crystal and that their symmetry lowers from A to C progressively.

Figure 4 shows the temperature dependence of the emission spectra excited at 210 nm. The A center emission lines at 678, 690, 718, 753 and 800 nm, associated with the $^5D_0 \rightarrow {}^7F_J$ (J = 0,1,2,3,4) transitions,

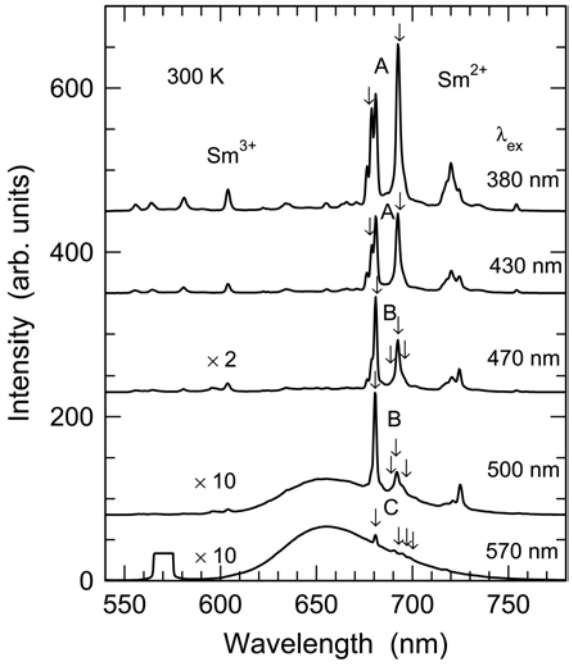

Fig. 5. Emission spectra excited at various wavelengths for KY_3F_{10} : 1%Sm at 300 K.

had intensities which decreased gradually with an increase of temperature. The intensities of the $^5D_3 \rightarrow {}^7F_J$ (J = 0,1,2,3,4) transitions at 489, 496, 510, 529 and 551 nm decreased rapidly up to 150 K and disappeared completely above 200 K. The weak intensities of the emission lines in the range of 550-620 nm, being due to the $^5D_2 \rightarrow {}^7F_J$ (J = 0,1,2,3,4) transitions of the A center, were almost constant at temperatures below 150 K, decreased as the temperature increased above 150 K and eventually disappeared at 300 K. At 300 K, the fairly weak emission lines remained at 560, 600 and 650 nm, being coincident with those due to Sm^{3+} as shown in Fig. 2. At 300 K, the weak emission lines of the A center around 700 nm due to the $^5D_0 \rightarrow {}^7F_J$ (J = 0,1,2,3,4) transitions were reduced to one-tenth of those observed at 10 K.

Above results suggest the following points. At low temperature, the excited electron in the higher energy $4f^5 5d$ excited state of the A center relaxes nonradiatively to the lower ^5D_J (J = 0,1,2,3) multiplets just below it, and is followed by radiative de-excitation to the lowest ^7F_J (J = 0,1,2,3,4) multiplets. As the temperature increases, the excited electron in the $^5D_3$ and $^5D_2$ multiplets de-excites nonradiatively to the metastable $^5D_0$ multiplet through phonon-assisted relaxation, then, the emission lines from the $^5D_3$ and $^5D_2$ multiplets disappear above 200 and 250 K, respectively, as shown in Fig. 4.

Figure 5 shows the emission spectra observed with various excitation wavelengths at 300 K. 380 nm excitation produced the same Sm^{3+} emission lines as in Fig. 3 and the A and B emission lines of Sm^{2+}. With an

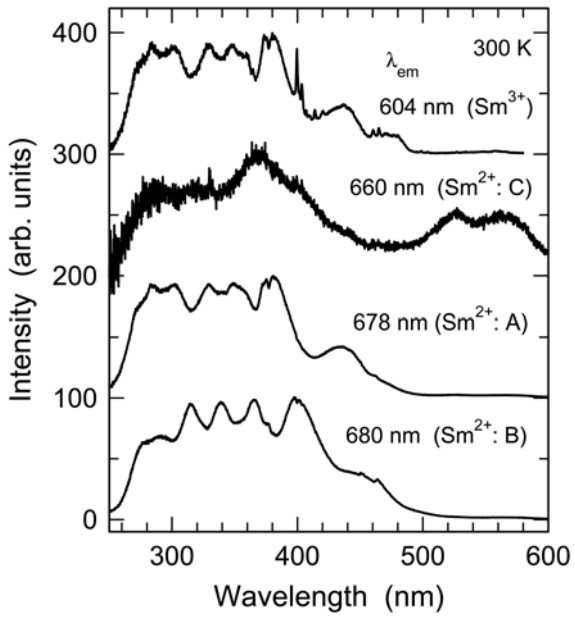

Fig. 6. Excitation spectra obtained by monitoring the intensities from the 604 nm lines of Sm^{3+}, the 678 nm (A) and 680 nm (B) lines of Sm^{2+}, and the 660 nm broadband in KY_3F_{10} : 1%Sm.

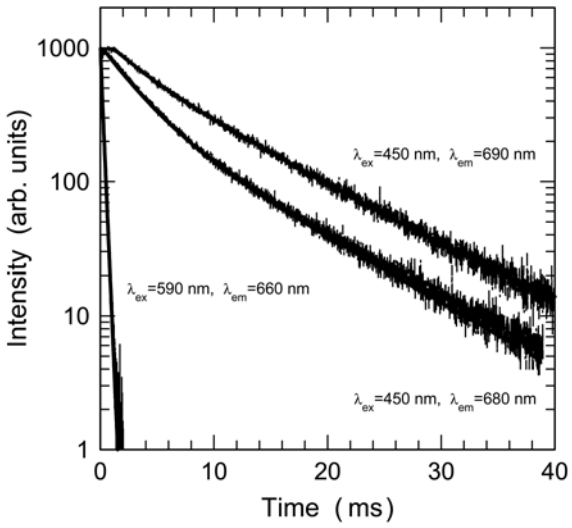

Fig. 7. Decay curves of the 690 and 680 nm lines excited at 450 nm and the 660 nm broadband excited at 590 nm when measured at 300 K. The decay curves fit curves calculated using $I(t) = 380 \times \exp(-t/3.0) + 850 \times \exp(-t/9.0)$, $I(t) = 700 \times \exp(-t/3.0) + 350 \times \exp(-t/.0)$, $I(t) = 900 \times \exp(-t/0.23)$, respectively.

increase of the excitation wavelength to 570 nm, a broad emission band appeared strongly. The A and B emission lines were not apparent, however, the $^5D_0 \rightarrow {}^7F_0$ and $^5D_0 \rightarrow {}^7F_1$ transitions of the C center were weakly observable. The broadband obtained at 300 K by the 570 nm excitation was not observed at 10 K as shown in Fig. 2. This fact suggests that the broadband is observable through thermal population into the higher lying $4f^5$5d excited state of the C center.

Figure 6 shows the selective excitation spectra obtained by monitoring the intensities of the 604 nm lines of Sm^{3+}, the 678 nm (A) and 680 nm (B) lines of Sm^{2+}, and the 660 nm broadband. The band structure of the excitation spectrum of the A center is almost the same as that of the absorption spectrum at 10 K in Fig. 1. This demonstrates that the absorption spectrum dominantly comes from the A center of Sm^{2+}. The band structure for the B center is shifted toward lower energy by about 1,200 cm^{-1}. On the other hand, the excitation spectrum of the 604 nm line ($^4G_{5/2} \rightarrow {}^6H_{7/2}$) of Sm^{3+} superimposes the bands due to the $4f^6 \rightarrow 4f^5$5d transitions of the A center on the sharp lines around 400 and 460 nm due to the $4f^5 \rightarrow 4f^5$ transitions of Sm^{3+}. This fact suggests energy transfer from Sm^{2+}(A) to Sm^{3+}. The excitation spectrum of the 660 nm broadband consists of the double-peaked bands at 528 and 560 nm, and unresolved broad bands similar to those of the A and B centers in the range of 260-460 nm. The double-peaked bands at 528 and 560 nm are completely coincident with those in the absorption spectrum at 10 K in Fig. 1. If these low energy bands are assumed to be due to the transitions to the lowest $4f^5$5d excited states of the C center, the energy separation between the energy levels of the lowest $4f^5$5d excited state and the $^5D_0$ multiplet of the C center is coincident with that (1300 cm^{-1}) estimated from the laser excitation spectrum of the C center at 10 K [5].

Figure 7 shows the decay curves of the 690 nm line due to the $^5D_0 \rightarrow {}^7F_1$ transition of the A center and the 680 nm line due to the $^5D_0 \rightarrow {}^7F_0$ transition of the B center when excited at 450 nm for a sample temperature of 300 K. These curves do not fit a single exponential function, however, are decomposed into two components. The same decay times of each 690 or 680 nm line can be estimated to be 3 and 9 ms with different initial intensities at $t = 0$, that is, the decay times of the dominant components of the 690 and 680 nm lines, corresponding to the A and B centers, are 9 and 3 ms, respectively. The short decay time for the B center, compared with that for the A center, means that the electric dipole transition for the B center is induced by an odd-parity distortion produced by the charge compensator. Another feature is the observation of a rise time in the 690 nm decay curve of the A center. This suggests energy transfer from the B to A center. The decay curve of the 660 nm broadband excited at 590 nm in Fig. 7 fits a single exponential function. The shorter decay time is estimated to be 230 μs. The optical transition, being parity-allowed by an electric dipole mechanism, may be derived from the $4f^5$5d excited state of the C center.

Figure 8 shows the emission spectra excited at 532 nm with various duration of irradiation for a sample temperature of 300 K. With increasing the irradiation times, the intensity of the 660 nm broadband markedly decreased. The intensity after 30 minutes became one-quarter of the initial intensity at $t = 0$. This

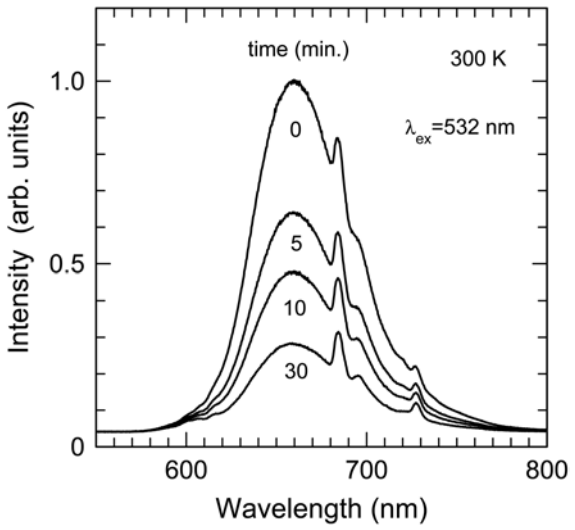

Fig. 8. Optical bleaching of the broadband emission in KY_3F_{10} : 1%Sm under continuous irradiation at 532 nm for a sample temperature of 300 K.

effect is called optical bleaching, which was observed for Sm^{2+} in fluoride crystals [9] and glasses [2].

Discussion

From the high resolution spectra of the $^5D_0 \rightarrow {}^7F_0$ and $^5D_0 \rightarrow {}^7F_1$ transitions of Sm^{2+}, we conclude the following three points: (i) the position of the $^5D_0 \rightarrow {}^7F_0$ line is red-shifted from 678.8 to 680.6 and 681.2 nm for the A, B and C centers, respectively; (ii) the splitting of the $^7F_1$ multiplet increases in magnitude for the A, B and C centers, respectively; and (iii) the intensity ratio of the $^5D_0 \rightarrow {}^7F_0$ line to the $^5D_0 \rightarrow {}^7F_1$ lines is 0.25, 1.3 and 1.0, for the A, B and C centers, respectively. These results suggest that the A center with high symmetry exhibits a magnetic dipole $^5D_0 \rightarrow {}^7F_0$ transition, whereas the B and C centers exhibit an electric dipole $^5D_0 \rightarrow {}^7F_0$ transition induced by an odd-parity distortion created by a nearby fluorine vacancy (V_F). The symmetry of the A, B and C centers is successively lowering in this series as evidenced by the increasing energy separation between the three $^5D_0 \rightarrow {}^7F_1$ lines.

This is reasonable assuming that substitution of Sm^{2+} on an Y^{3+} site provides a C_{4v} symmetry electrostatic potential and that it is possible that a V_F center is only a slight perturbation upon Sm^{2+}. The A center having close to C_{4v} symmetry, is assigned to a Sm^{2+} ion with its charge compensating V_F at a relatively long distance. However, the B and C centers have a greater 'non-centrosymmetric' crystal-field than the A center. Such an odd-parity crystal field mixes opposite parity wavefunctions into the $^5D_0$ multiplets of the B and C centers, resulting in breakdown of the parity selection rule.

We discuss the energy transfer from the A center of Sm^{2+} to Sm^{3+} as shown in Fig. 6. The energy level (17,870 cm^{-1}) of the metastable $^4G_{5/2}$ multiplet of Sm^{3+} is just below those (18,037 and 17,990 cm^{-1}) of the $^5D_2$ multiplets of the A and B centers of Sm^{2+}, respectively. Cascade emission from the $^5D_3$ and $^5D_2$ multiplets was observed only for the A center, but not for the B center. It might be expected that the decay time of the $^5D_2$ multiplet of the A center is long compared with that for the B center. As a consequence, the A center has two relaxation paths to the lower $^5D_1$ and $^5D_0$ multiplets of Sm^{2+} and the metastable $^4G_{5/2}$ multiplet of Sm^{3+}. On the other hand, the B center has only a single relaxation path directly to its own metastable $^5D_0$ multiplet. The relaxation time from the $^5D_2$ multiplet of the B center may become shorter because of the small energy separation between the $^5D_2$ multiplet and the lower $4f^55d$ excited state.

Next, we consider the origin of the 660 nm broadband emission, which was not observed at 10 K, but at 300 K, as shown in Figs. 2 and 5. A model is the C center of Sm^{2+} perturbed by a nearby V_F center [5, 10]. The energy level of the lowest $4f^55d$ excited state for the C center was estimated to lie just above the $^5D_0$ multiplet by 1,300 cm^{-1} [5]. As the temperature increases, part of the excited electrons lying on the metastable $^5D_0$ multiple are thermally populated to the higher $4f^55d$ excited state, resulting in that the broadband emission with the short decay time of 230 μs are observable at 300 K as shown in Fig. 5 because of the parity-allowed $4f^55d \rightarrow 4f^6$ transition.

Finally, we consider a mechanism of the optical bleaching of the 660 nm broadband emission as shown in Fig. 8, on the assumption that the broadband is emitted from the higher $4f^55d$ excited state of the C center. In general, optical bleaching follows energy transfer from a radiative center to a nonradiative center. Here, the nonradiative center is assumed to be a V_F center near to Sm^{2+}. Continuous irradiation converts a complex of Sm^{2+} and V_F to that of Sm^{3+} and *F*-center, being a single electron trapped at V_F [11]. This model leads to both reduction of the broad emission band and the sharp emission lines of the C center and enhancement of the sharp emission lines of Sm^{3+} and another broadband emission of the *F*-center. However, such reduction and enhancement were not observed in the emission spectra in Fig. 8. The other possible model is an isolated *F*-center. Although this model can explain optical bleaching of the broadband, it is difficult to explain the temperature behavior of the broadband emission. Therefore, in order to understand the optical bleaching mechanism, we have to do further experiments, for example, temperature dependence of the decay curves and the optical bleaching of the broad emission band excited at 590 nm as shown in Figs. 7 and 8.

Acknowledgments

This work was supported by the Use-of-UVSOR Facility Program (No. 25-515) of the Institute for Molecular Science. T. P. J. Han would like to acknowledge the financial support of EPSRC, UK. J.-P. R. Wells would like to acknowledge for the support of the Marsden Fund of the Royal Society of New Zealand under contact 09-UOC-080.

References

1. G. Blasse and B.C. Grabmaier, Luminescent Materials (Springer-Verlag, Berlin, 1994).
2. A. Osvet, S. Emelianova, R. Weissmann, V.I. Arbuzov, A. Winnacker, J. Lumin. 86 (2000) 323-332.
3. X. Xue, M. Liao, R. N. Tiwari, M. Yoshimura, T. Suzuki, Y. Ohishi, Appl. Phys. Express 5 (2012) 092601-3.
4. P. Porcher and P. Caro, J. Chem. Phys. 65 (1976) 89-94.
5. J.-P.R. Wells, A. Sugiyama, T.P.J. Han, and H.G. Gallagher, J. Lumin. 85 (1999) 91-102.
6. M. Yamaga, T. Nakamura, Y. Oda, J.-P.R. Wells, and T.P.J. Han, J. Ceram. Process. Res. Special 3 (2011) S241-S245.
7. E. Radzhabov, J. Phys.: Condens. Matter 13 (2001) 10955-10967.
8. K. Shimamura, S. Baldochi, I.M. Ranieri, H. Sato, T. Fujita, V.L. Mazzocchi, C. B.R. Parente, C.O. Paiva-Santos, C.V. Santill, N. Sarukura, and T. Fukuda, J. Crystal Growth 223 (2001) 383-388.
9. K. Ito, M. Yamaga, N. Kodama, J. Alloys and Comp. 408-412 (2006) 766-770.
10. L.C. Dixie, A. Edgar, M.F. Reid, J. Lumin. 132 (2012) 2775-2782.
11. J.J. Markham, F-centers in alkali halides (Academic Press, New York, 1966).